The changing impact mechanisms of a diverse El Niño on the Western Pacific Subtropical High

Mengyan Chen[1,2,3], Jin-Yi Yu[3], Xin Wang[1,4*], Wenping Jiang[5]

[1] State Key Laboratory of Tropical Oceanography, South China Sea Institute of Oceanology, Chinese Academy of Sciences, Guangzhou 510301, P. R. China

[2] University of Chinese Academy of Sciences, Beijing 100049, P. R. China

[3] Department of Earth System Science, University of California, Irvine, California, USA

[4] Laboratory for Regional Oceanography and Numerical Modeling, Qingdao National Laboratory for Marine Science and Technology, Qingdao 266237, P. R. China

[5] College of Oceanography, Hohai University, Nanjing 210098, P. R. China

* Corresponding authors: Xin Wang (wangxin@scsio.ac.cn)

This article has been accepted for publication and undergone full peer review but has not been through the copyediting, typesetting, pagination and proofreading process which may lead to differences between this version and the Version of Record. Please cite this article as doi: 10.1029/2018GL081131

Three key points:

1. El Niño diversity invokes NW Pacific coupling, Indian Ocean capacitor, and MC mechanism to produce distinct impacts on WPSH.
2. The changing importance of these mechanisms is caused by different SST anomaly in Pacific and Indian Oceans during various El Niño types.
3. The different impacts indicate that CP-I and CP-II El Niños are forced by Indian Ocean and extratropical Pacific, respectively.

ABSTRACT

The composite analyses during 1950-2016 show that the impacts of El Niño on the western Pacific subtropical high (WPSH) are different among the Eastern Pacific (EP) type, Central Pacific type-I (CP-I), and Central Pacific type-II (CP-I). The three types of El Niño produce distinct impacts on WPSH due to the varying importance of the Northwestern Pacific coupling, Indian Ocean capacitor, and Maritime Continent mechanisms. The different enhancements and cancellations among these three mechanisms are related to differences in SST anomaly locations and Indian Ocean conditions among the El Niño types. The CP-II El Niño becomes the most influential type of El Niño, while the CP-I El Niño becomes the least influential type. The different impacts and mechanisms for the CP-I and CP-II types of El Niño imply that these two sub-types of CP El Niño may involve different forcing from the Indian Ocean and extratropical Pacific for their generation.

Key words: western Pacific subtropical high; EP El Niño; CP-I El Niño; CP-II El Niño

Plain Language Summary

It is now well recognized that there exists a conventional Eastern Pacific (EP) type and an emerging Central Pacific (CP) type of El Niño. Recent studies have suggested that the CP El Niño should be further separated into two subtypes. It is shown here that these three ENSO types produce distinct impacts on the Western Pacific Subtropical High (WPSH). The conventional views of El Niño's impacts on the WPSH and their underlying mechanisms need to be revised to take into account of the El Niño diversity. This study also offers new insights into the generation dynamics of the two subtypes of the CP El Niño. We find that the two subtypes of CP El Niño differ not only in their sea surface temperature anomalies in the northeastern Pacific but also in the Indian Ocean.

1. Introduction

El Niño is the strongest interannual variation in sea surface temperature (SST) in the tropical Pacific, and its impacts on global climate have been extensively studied (e.g., Rasmusson & Carpenter, 1982; Trenberth et al., 1998; Lyon et al., 2005; Yu et al., 2012; Yuan & Yang, 2012; Wang & Wang, 2013, 2014; Liu et al. 2014; Wang et al. 2014; Yang et al. 2018). The conventional views on El Niño impacts began to be revised recently due to the recognition that El Niño has different types and their climate impacts can be different (e.g., Harrison & Chiodi, 2015; Yu et al., 2012, 17; and Capotondi et al., 2015 for a review by US CLIVAR ENSO Diversity Working Group). Studies on El Niño diversity often classify the El Niño into two types based on the zonal location of their maximum positive SST anomalies, which are often referred to as the Eastern Pacific (EP) and Central Pacific (CP) El Niño (Yu & Kao, 2007; Kao & Yu, 2009). The EP El Niño has most of its SST anomalies located in the eastern Pacific, while the CP El Niño has most of its SST anomalies located in the central Pacific. The CP type is similar to El Niño Modoki (Ashok et al., 2007) in SST anomaly structures, and these two terms have both been used to refer to this type of El Niño. A recent study by Wang and Wang (2013) suggested that the Modoki type needs to be further separated into Modoki-I and II, due to the different evolutions of their SST anomalies and different climate impacts they produce. An index was also developed to identify these two types of El Niño Modoki (Wang et al., 2018a). For the sake of simplicity, we refer to Modoki-I and II as CP-I and CP-II, respectively, in this study. While these two types of CP El Niño are similar in having their largest SST anomalies located in the tropical central Pacific, their origins and spatial patterns of positive SST anomalies are very different. The positive

SST anomalies associated with the CP-I El Niño originate at the equator and are more symmetric about the equator, while the SST anomalies associated with the CP-II El Niño are additionally characterized by positive SST anomalies extending from the tropical central Pacific towards the North American Coast during its developing phase and that are asymmetric about the equator during the peak phase. These two subtypes of CP El Niño have been shown to produce opposite impacts on typhoon activities, rainfall in southern China (Wang & Wang, 2013), the Indian Ocean Dipole (Wang & Wang, 2014), and the South China Sea SST anomalies (Tan et al., 2016).

The Western Pacific subtropical high (WPSH) is a key feature of Asian-Pacific climate. Variations in the location and intensity can influence the strengths of the East Asian monsoon (e.g., Chang et al., 2000; Wang et al., 2000; Lee et al., 2005; Park et al., 2010) and Indian summer monsoon (ISM) (Huang et al., 2018) as well as the tracks of western Pacific typhoons (e.g., Ho et al., 2004; Wu et al., 2005; Du et al., 2011). Previous reviews have summarized the impact on the WPSH of tropical SST anomalies (He et al., 2015; Li et al., 2017). Forcing from El Niño is a key source of WPSH variability. The El Niño impact on the WPSH has been intensively studied (e.g., Wang et al., 2000; Wang & Zhang, 2002; Kumar & Hoerling, 2003; Sui et al., 2007; Xie et al., 2009, 2016**;** He et al., 2015; Park et al., 2010; Yuan et al., 2012; Paek et al., 2015, 2016; Li et al., 2017; Jiang et al., 2017, 2018), and the prevailing view is that the WPSH typically intensifies during the decaying summer of El Niño (e.g., Wang et al., 2000; Xie et al., 2009, Xiang et al., 2013). A northwestern Pacific (NWP) local coupling mechanism (Wang et al., 2000) and an Indian Ocean Capacitor (IOC) mechanism (Xie et al., 2009) were proposed to explain how El Niño can still influence the

WPSH intensity after its demise. The NWP mechanism suggests that NWP SST anomalies induced by El Niño during its developing phase can sustain themselves via local atmosphere-ocean coupling through the following seasons, and act to intensify the WPSH. The IOC mechanism suggests that the tropical Indian Ocean warming induced by El Niño during its developing phase acts like a capacitor to sustain the El Niño influence into the following summer and influences the WPSH via Kelvin wave-induced Ekman divergence. A third mechanism related to the Maritime Continent (MC) has also been put forward to link El Niño to the WPSH (Sui et al., 2007). In this mechanism, MC SST anomalies induced by El Niño can affect the WPSH intensity through the regional Hadley circulation connecting the MC and WPSH regions.

These impact mechanisms were proposed before the diversity in El Niño types was fully recognized by the research community. Recent studies have examined whether and how the different types of El Niño impact the WPSH differently (e.g., Paek et al., 2015, 2016) by separating the El Niño only into the EP and CP types. In this study, we show with observational analyses that CP El Niño impacts on the WPSH are different between CP-I and CP-II subtypes. The distinct impacts and the underlying impact mechanisms of these three types of El Niño on the WPSH are identified and described in this study. The findings also provide some interesting insights into the possible differences in the underlying generation dynamics for the two subtypes of CP El Niño.

2. Data and methods

The observational datasets used in this study include monthly SST from the Hadley

Centre Sea Ice and SST dataset (HadISST) with a 1.0°×1.0° horizontal resolution (Rayner et al., 2003) and monthly sea level pressures (SLP), surface winds and vertical velocities at a horizontal resolution of 2.5°×2.5° obtained from the National Centers for Environmental Prediction/National Center for Atmospheric Research (NCEP/NCAR) Reanalysis 1 (Kalnay et al., 1996). Years 1950-2016 are analyzed in this study. Anomalies are defined as the deviations from the climatological mean over the entire period. Linear trends are removed in this study. Years (0) and (1) are used to refer to the developing and decaying years of El Niño, respectively.

A composite analysis was performed in this study for the three types of El Niño. Based on the three El Niño types identified by Wang and Wang (2013), seven EP El Niño (1951/1952, 1965/1966, 1972/1973, 1976/1977, 1982/1983, 1997/1998, 2015/2016), four CP-I (1963/1964, 1987/1988, 1990/1991, 2002/2003), and six CP-II (1968/1969, 1979/1980, 1991/1992, 1992/1993, 2004/2005, 2009/2010) were selected for this analysis.

3. Results

To represent the WPSH intensity, we define a WPSH index as the SLP anomalies averaged over the northwestern Pacific region (10°-30°N, 120°-160°E) following Paek et al. (2015). We compare in Figure 1 the evolution of this WPSH index composited for the three types of El Niño from their developing May to decaying August. The values have been normalized by their respective standard deviation and smoothed with a 3-month running average to reduce the effect of intra-seasonal variability. Our examinations focus on the developing summer (from June to August), developing winter (December to February), and

decaying summer (from June to August). The seasons correspond to the typical developing, mature, and decaying phases of El Niño. The figure indicates that the three types of El Niño impact the WPSH in very different ways. El Niño (Figure 1a) produces strong (≥0.5 standard deviation) impacts on the WPSH during the developing winter and decaying summer for the EP type (Figure 1a), only during the developing winter for the CP-I type (Figure 1b), and throughout the developing late summer (August and September), developing winter, and decaying summer for the CP-II type (Figure 1c). Apparently, the CP-II is the El Niño type that is most capable of influencing the WPSH, while the impacts from CP-I are the weakest. The distinct impacts further support the suggestion of separating the CP El Niño into the CP-I and CP-II subtypes. All three types of El Niño can impact the WPSH during boreal winter when the El Niños reach their peak intensity. The impacts differ the most during the developing and decaying summers. Figure 1 also indicates that, regardless of the type, El Niño impacts on the WPSH intensity are mostly negative (i.e., weakening) during the developing summer but positive (i.e., strengthening) during the decaying summer (e.g., EP and CP-II).

We next examine if different mechanisms are invoked to produce the distinct impacts on the WPSH during different seasons. We use four indices to examine the strengths of the three impact mechanisms: an MC index for the regional Hadley circulation mechanism connecting the MC and WPSH regions, a north Indian Ocean (NIO) index for the IOC mechanism, a tropical central Pacific (TCP) index and a subtropical central Pacific (SCP) index for the NWP local air-sea coupling mechanism. The regions used to define these indices are indicated in Figure 2. These regions were either adopted from previous studies or based on

results from previous studies. Based on the results of Sui et al. (2007), we define a MC index to quantify the strength of the regional meridional circulation using the 850-hPa vertical velocity differences between the maritime continent region (20°S-10°N, 110°-150°E) and the WPSH index region. Positive values of the MC index represent anomalous ascent from the MC region and anomalous descent over the WPSH region and vice versa for negative values. Following Xie et al. (2016), we define a NIO index to quantify the Indian Ocean warming or cooling during El Niño as the SST anomalies averaged over the tropical north Indian Ocean (5-25°N, 40°-100°E). The NWP local coupling mechanism involves interactions between NWP SST anomalies and the overlaying anomalous cyclonic or anticyclonic circulation induced by El Niño. As described in Wang et al. (2000), warm SST anomalies in the tropical eastern Pacific during a conventional El Niño (i.e., EP El Niño) can excite a Gill-type response that produces an anomalous cyclone to the west. This anomalous cyclone then intensities the background trade winds resulting in negative SST anomalies in the subtropical central Pacific. It is these cold SST anomalies that induce a second Gill type response resulting in the anomalous anticyclone involved in the NWP local coupling mechanism. Following Xie et al. (2016), we define the SST anomalies averaged over this subtropical central Pacific (10-20°N, 150°-170°E) as the SCP index to quantifying the NWP local-coupling mechanism related to this two-step Gill response. However, SST anomalies in the Niño4 region can also directly induce an anomalous cyclone or anticyclone over the NWP region via a one-step Gill response (Fan et al., 2013) to produce the same NWP local-coupling mechanism. Following Fan et al. (2013), we additionally define a TCP index as the SST anomalies averaged over the tropical central Pacific Ocean (10°S-10°N,

160°-180°E) multiply -1 to quantify the NWP local-coupling mechanism through this one-step Gill response process. The -1 multiplication is to reflect the fact that warm (cold) SST anomalies in the TCP region can induce negative (positive) WPSH index via the one-step Gill type response. As we will show later it is important to consider both the one-step and two-step Gill response processes in order to fully understand the NWP local-coupling mechanism during EP and CP El Niño events. We will refer to the NWP local coupling mechanism produced by the one-step and two-step Gill responses as the NWP-TCP mechanism and NWP-SCP mechanism, respectively. We also perform additional regression and composite analyses (see Supplementary Text S1) with SST (Figure S1), precipitation (Figure S2), and outgoing longwave radiation (OLR; Figure S3) anomalies to demonstrate that these four index regions reasonably coincide with and represent the central heating or ascending/descending regions associated with the impact mechanisms. Therefore, the four mechanism indices are reasonably defined.

We composite these four mechanism indices for the three El Niño types and superimpose them on the WPSH index in Figure 1. Similar to the WPSH index, all values are smooth and normalized to facilitate comparisons. Figure 1a shows that, consistent with the conventional view (e.g., Wang et al. 2000), the NWP local-coupling mechanism is a key process by which the EP El Niño impacts the WPSH. The local-coupling is produced mostly by the positive SST anomalies in the tropical eastern Pacific through the two-step Gill response process. Values of the SCP index are large and positive throughout most of the lifecycle of the EP El Niño, particularly during the peak winter. The one-step Gill process related to SST anomalies in the tropical central Pacific contributes little to the NWP local

coupling, which is evident by the small values of the TCP index throughout the lifecycle of EP El Niño. From the Supplementary Figures, we find that the SCP index regions mostly coincide with regions of large negative (positive) precipitation anomalies and positive (negative) OLR anomalies during the decaying phase of EP and CP-II El Niño (CP-I El Niño) (Figures S2 and S3). TCP index regions mostly coincide with regions of positive precipitation anomalies and negative OLR anomalies during the decaying phase of all three types of El Niño (Figures S2 and S3). Also consistent with the conventional view suggested by Xie et al. (2009), the IOC mechanism is another key process by which the conventional EP El Niño acts to intensify the WPSH. Our Supplementary figures show that the TIO index region we selected reasonably represents the region of large positive precipitation anomalies (Figure S2c) and large negative OLR anomalies (Figure S3c) during the decay phase of the EP El Niño. Values of the IOC index begin to increase after the El Niño develops during summer and maintain large positive values through the developing winter to decaying summer. Figure 1a shows that NWP-SCP local coupling and IOC mechanisms work together to enable the EP Niño to produce a delayed impact on the WPSH during the decaying summer. The NWP-SCP mechanism is also large during the developing summer but its effects are mostly canceled out by the negative impacts produced by the MC mechanism resulting in a weak impact of the EP El Niño on WPSH. During this season, the Indian Ocean has not been charged ("warmed up") enough to produce a strong IOC mechanism. As for the MC mechanism, it also contributes to the delayed summer impact on the WPSH. The variations in the four mechanism indices are consistent with the established understanding of how the EP El Niño impacts the WPSH during different seasons. This analysis demonstrates that the four mechanism indices we

defined are useful in quantifying and understanding the impact mechanisms of El Niño on the WPSH.

Figures 1b and c show that, for both CP-I and CP-II El Niño, the one-step Gill process replaces the two-step Gill process in the local coupling in the NWP region. Values of the TCP index are large and negative throughout most of the lifecycle for these two El Niño types, while values of the SCP index are smaller than those associated with EP El Niño. The differences between these two Gill processes are related to the fact that the central location of SST anomalies moves from the tropical eastern Pacific during EP El Niños to the tropical central Pacific during CP-I and CP-II El Niños. This can be seen from Figure 2, which shows the evolutions of SST anomalies composited for three types. The figure clearly show that the positive SST anomalies appear, develop, and decay more in the tropical eastern Pacific for EP El Niño (Figures 2a-f) but more in the tropical central Pacific for CP-I (Figures 2g-l) and CP-II (Figures 2m-r). The former SST anomaly location triggers the two-step Gill process whereas the latter SST anomaly location triggers the one-step Gill process. Since the one-step Gill response excites an anomalous cyclonic circulation (rather than an anomalous anticyclone as in the two-step Gill response) over the WNP region, this mechanism works to weaken the WPSH. This mechanism enables both subtypes of CP El Niño to produce a negative impact on the WPSH during the developing summer. However, this negative impact is mostly cancelled out by the IOC mechanism throughout the lifecycle of CP-I El Niño and by the MC mechanism during the latter phases (i.e., developing winter and decaying summer) of CP-II El Niño.

It is interesting to note that, similar to the EP Niño, the IOC mechanism is strong for

CP-I El Niño, but is weak for CP-II El Niño. The CP-II is the only El Niño type for which the IOC mechanism is weak. This is because SST anomalies in the Indian Ocean during this type are much smaller than those during the CP-I El Niño and EP types, which is evident in Figure 2. Yu et al. (2015) argued that the more-westward located SST anomalies render the CP El Niño less capable than the EP El Niño of disturbing the Pacific Walker circulation, one result of this is that smaller SST anomalies are induced by CP El Niño in the Indian Ocean. We find their argument to be particularly true for the CP-II El Niño but not for the CP-I El Niño. This then raises the question of why the CP-I can be accompanied by significant SST anomalies in the Indian Ocean? We notice that significant Indian Ocean warming already exists during MAM(0) (Figure 2g), before the CP-I El Niño develops fully. This is very different from the Indian Ocean warming associated with the EP El Niño that tends to occur after the El Niño fully developed (see Figures 2 a-f). We can see from Figure 1b that the IOC index already has large values before the developing summer of the CP-I El Niño, whereas the IOC index is still small for EP El Niño during that season (Figure 1a). Also, the typical Indian Ocean Dipole pattern induced by the EP El Niño during the developing phase (e.g., JJA(0) in Figure 2b) does not appear during the CP-I El Niño. The Indian Ocean warming associated with EP El Niño is known to be a response to the El Niño and lags its development. However, for the CP-I El Niño, the Indian Ocean warming does not look like a response, but rather a precursor. Our analyses suggest that the Indian Ocean warming may be involved in the onset mechanism of the CP-I El Niño. An earlier study by Yu et al. (2009) has already suggested that CP El Niño can also be forced by anomalies winds associated with the Indian monsoon. It is possible that the CP-I El Niño is associated with the forcing from Indian ocean and/or

monsoon (Yu et al., 2009), while the CP-II El Niño is associated with forcing from the extratropical Pacific (Yu et al., 2010; Yu & Kim, 2011; Yu et al., 2017; Wang et al., 2018b). This might be the reason why the CP-II is associated with SST precursors (i.e., warming) extending from the northeastern Pacific to the tropical central Pacific (see Figures 2m and n) whereas the CP-I is associated with SST precursors in the Indian Ocean (see Figures 2g and h). Further research is needed to confirm this possibility.

The different evolutions of Indian Ocean SST anomalies among the three El Niño types can also explain the differing relative importance of the MC mechanism in producing the impacts on the WPSH. We notice from Figure 1 that, in general, the MC index switches from negative values during the developing summer to positive values during the decaying summer. This index is particularly strong during the decaying summer for the CP-II El Niño, which enables this type of El Niño to produce a delayed impact on the WPSH. This delayed impact mechanism is unique to the CP-II because it is the only El Niño type that is not associated with large SST anomalies in the Indian Ocean during the decaying summer. As shown in Figure 2q, significant SST anomalies associated with the CP-II El Niño are isolated around the MC region during the decaying summer with no significant anomalies in large parts of the Indian Ocean. The isolated warm SST anomalies induce strong anomalous surface convergence over the MC, which can be seen in the composited 1000-hPa velocity potential anomalies shown in Figure 3i. The figure shows that the positive (i.e., convergence) anomaly center over the MC is accompanied by a negative (i.e., divergence) anomaly center over the WPSH. This figure indicates that the anomalous MC convergence (and ascent) can induce anomalous descent over the WPSH via the regional meridional circulation mechanism (Sui et

al., 2007). The composited surface wind anomalies in Figure 3i show an anticyclonic circulation over the WPSH region, consistent with the strengthened WPSH during the decaying summer in Figure 1c. This mechanism is also present during the EP type of El Niño, because EP El Niños have large SST anomalies in the Indian Ocean during the decaying summer and the warm SST anomalies extend into the MC region (Figure 2f), leading to a strong convergence anomaly center over the Indian Ocean and MC and a divergence anomaly center over the WPSH (Figures 3c). This mechanism is not present during the CP-I type of El Niño because this type has large positive SST anomalies in the Indian Ocean during the decaying summer (see Figures 2l), which overwhelm the MC SST anomalies, shifting the anomalous ascent from the MC to the Indian Ocean (Figures 3f). Therefore, the MC mechanism becomes weak for the CP-I El Niños during their decaying summer (see Figures 1b). During the CP-I El Niño, TIO warm SST anomalies can still excite a Kelvin wave to influence the WPSH region. However, this effect is cancelled out by a two-step Gill type response to the cold SST anomalies that develop in the equatorial eastern Pacific (see Figure 2l). This cancellation effect is suggested by the mechanism indices in Figure 1b. Due to this cancellation effect, the circulation anomalies induced by the TIO warm SST anomalies is limited to the region immediately to the northeast over the Bay of Bengal (see surface wind vectors shown in Figure 3f). During the developing winter, Figures 3b, e, and h show that the zonal Walker circulation dominates the near surface anomalous ascent and descent. The MC meridional circulation mechanism is relatively weak during this season for all three El Niño types (see Figure 1).

4. Conclusions and discussion

In this study, we showed via observational analyses that the EP, CP-I, and CP-II types of El Niño produce distinct impacts on the WPSH via different combinations of the impact mechanisms. Figure 4 summaries the key impact mechanisms identified from the study. For simplicity, the illustration emphasizes the processes at work during the decaying summer of the El Niños. The figure indicates that the more westward-located warm SST anomalies during the CP-I and CP-II types result in a NWP local coupling that is dominated by the one-step Gill response rather than the two-step Gill response associated with the EP El Niño (Figure 4a). The two-step Gill response is also involved in exerting negative impacts on WPSH for the CP-I El Niño because of the cold anomalies appeared in the eastern Pacific. As a result, the NWP local coupling mechanism no longer works to intensify but instead weakens the WPSH. These negative effects cancel out the intensification impact from the IOC mechanism resulting in a weak or non-existent impact of the CP-I El Niño (Figure 4b) during the decaying summer. However, the CP-II El Niño can still produce a delayed impact on WPSH during this season due to the strong positive impact produced by the MC mechanism (Figure 4c). The MC mechanism is uniquely strong for the CP-II because it is the only El Niño type that neither forces nor is preceded by large SST anomalies in the Indian Ocean. As a result of the superposition and cancellation of these three impact mechanisms, the CP-II El Niño is the most influential type of El Niño on the WPSH whereas CP-I El Niño is the least. Our study shows that the conventional views of the El Niño impacts on WPSH and its underlying mechanisms need to be revised for different types of El Niño.

The findings reported in this study not only add support for the need to separate CP El

Niño into two subtypes but also offer new insights into the generation dynamics of the two subtypes. It is very important to recognize that the CP-I and CP-II differ not only in their SST anomalies in the Northeastern Pacific (which has been emphasized by Wang and Wang (2013) when they first identified these two subtypes) but also in their SST anomalies in the Indian Ocean. The CP-II El Niño is associated with very weak inter-basin interactions with the Indian Ocean, which is consistent with the explanation given in Paek et al. (2016). However, the CP-I El Niño is associated with very strong inter-basin interactions with the Indian Ocean. Therefore, it is possible that the CP-II El Niño is a Pacific-only phenomenon while the CP-I El Niño invokes involves the Indian Ocean and should be considered as an Indo-Pacific phenomenon. The reasons behind the different linkages with the Indian Ocean for the different types of El Niño deserves further study.

Acknowledgments. We thank two anonymous reviewers for their constructive comments. This research is supported by the Strategic Priority Research Program of Chinese Academy of Sciences (Grant No. XDA20060502), NSF Climate & Large-scale Dynamics Program under grants AGS1505145 and AGS-1833075, National Natural Science Foundation of China (Grant No. 41876021), the Fundamental Research Funds for the Central Universities (Grant No. 2018B08314) and China Scholarship Council. The SST data of Hadley Center Sea Ice and Sea Surface Temperature data set were downloaded from their site (http://www.metoffice.gov.uk/hadobs/hadisst/data/download.html). The monthly SLPs, winds and Omega fields of National Centers for Environmental Prediction/National Center for Atmospheric Research (NCEP–NCAR) were from NOAA (http://www.esrl.noaa.gov/psd/)

References

Ashok, K., Behera, S. K., Rao, S. A., Weng, H., & Yamagata, T. (2007). El Niño Modoki and its teleconnection. *Journal of Geophysical Research, 112,* C11007. https://doi.org/10.1029/2006JC003798

Capotondi, A., Wittenberg, A. T., Newman, M., Di Lorenzo, E., Yu, J. Y., Braconnot, P., et al. (2015). Understanding ENSO diversity. *Bulletin of the American Meteorological Society, 96*(6), 921–938. https://doi.org/10.1175/BAMS-D-13-00117.1

Chang, C. P., Zhang, Y., & Li, T. (2000). Interannual and interdecadal variations of the East Asian summer monsoon and tropical Pacific SSTs. Part I: Roles of the subtropical ridge. *Journal of Climate, 13,* 4310–4325. https://doi.org/10.1175/1520-0442(2000)013,4310: IAIVOT.2.0.CO;2

Du, Y., Yang, L., & Xie, S. P. (2011). Tropical Indian Ocean influence on Northwest Pacific tropical cyclones in summer following strong El Niño. *Journal of Climate, 24,* 315–322. https://doi.org/10.1175/2010JCLI3890.1

Fan, L., Shin, S. I., Liu Q. Y., & Liu, Z. Y. (2013). Relative importance of tropical SST anomalies in forcing East Asian summer monsoon circulation. *Geophysical Research Letters, 40,* 2471-2477. https://doi.org/10.1002/grl.50494

Harrison, D.E., & Chiodi A.M. (2015). Multi-decadal variability and trends in the El Niño-Southern Oscillation and tropical Pacific fisheries implications. *Deep-Sea Res. II,* 113. https://doi.org/10.1016/j.dsr2.2013.12.020, 9–21

He, C., Zhou, T., &Wu, B. (2015). The Key Oceanic Regions Responsible for the Interannual Variability of the Western North Pacific Subtropical High and Associated Mechanisms.

Journal of Meteorological Research, *29* (4):562-575. https://doi.org/10.1007/s13351-015-5037-3

Ho, C. H., Baik, J.J., Kim, J. H., Gong, D. Y., & Sui, C. H. (2004). Interdecadal changes in summertime typhoon tracks. *Journal of Climate*, *17*, 1767–1776. https://doi.org/10.1175/1520-0442(2004)017,1767: ICISTT.2.0.CO;2

Huang, Y., Wang, B., Li, X., & Wang, H. (2018). Changes in the influence of the western Pacifc subtropical high on Asian summer monsoon rainfall in the late 1990s. *Climate Dynamics, 51*, 443-455. https://doi.org/10.1007/s00382-017-3933-1

Jiang, W., Huang, G., Hu, K., Wu, R., Gong, H., Chen, X., & Tao, W. (2017). Diverse relationship between ENSO and the northwest Pacific summer climate among CMIP5 models: Dependence on the ENSO decay pace. *Journal of Climate, 30,* 109–127. https://doi.org/10.1175/JCLI-D-16-0365.1

Jiang, W., Huang, G., Huang P., & Hu, K. (2018). Weakening of Northwest Pacific Anticyclone Anomalies during Post–El Niño Summers under Global Warming. *Journal of Climate*, *31*, 3539-3555. https://doi.org/10.1175/JCLI-D-17-0613.1

Kalnay, E., Kanamitsu, M., Kistler, R., Collins, W., Deaven, D., Gandin, L., et al. (1996). The NCEP/NCAR 40-Year Reanalysis Project. *Bulletin of the American Meteorological Society*, *77*(3), 437–471. https://doi.org/10.1175/1520-0477(1996)077<0437:TNYRP>2.0.CO;2

Kao, H. Y., & Yu, J. Y. (2009). Contrasting eastern-Pacific and central-Pacific types of ENSO. *Journal of Climate, 22,* 615–632. https://doi.org/10.1175/2008JCLI2309.1

Kumar, A., & Hoerling, M. P. (2003). The nature and causes for the delayed atmospheric response to El Niño. *Journal of Climate, 16,* 1391–1403.

https://doi:10.1175/1520-0442-16.9.1391

Lee, E. J., Jhun, J. G., & Park, C. K. (2005). Remote connection of the northeast Asian summer rainfall variation revealed by a newly defined monsoon index. *Journal of Climate, 18,* 4381–4393. https://doi.org/10.1175/JCLI3545.1

Li, T., Wang, B., Wu, B., & Zhou, T. (2017). Theories on Formation of an Anomalous Anticyclone in Western North Pacific during El Niño: A Review. *Journal of Meteorological Research, 31* (6):987-1006. https://doi.org/10.1007/s13351-017-7147-6

Liu, Q.-Y., Wang, D., Wang, X., Shu, Y., Xie, Q., & Chen, J. (2014) Thermal variations in the South China Sea associated with the eastern and central Pacific El Niño events and their mechanisms. *J. Geophys. Res. Oceans,* 119, 8955-8972. https://doi.org/10.1002/2014JC010429

Lyon, B., & Barnston A. G. (2005). ENSO and the spatial extent of interannual precipitation extremes in tropical land areas. *Journal of Climate, 18,* 5095-5109. https://doi.org/10.1175/JCLI3598.1

Paek, H., Yu, J. Y., Hwu, J. W., Lu, M. M., & Gao, T. (2015). A source of AGCM bias in simulating the western Pacific subtropical high: different sensitivities to the two types of ENSO. *Monthly weather review. 143,* 2348–2362. https://doi.org/10.1175/MWR-D-14-00401.1

Paek, H., Yu, J. Y., Zheng, F., & Lu, M. M. (2016). Impacts of ENSO diversity on the western Pacific and North Pacific subtropical highs during boreal summer. *Climate Dynamics.* https://doi.org/10.1007/s00382-016-3288-z

Park, J. Y., Jhun, J. G., Yim, S. Y., & Kim W. M. (2010). Decadal changes in two types of the

western North Pacific subtropical high in boreal summer associated with Asian summer monsoon/El Niño–Southern Oscillation connections. *Journal of Geophysical Research, 115,* D21129. https://doi.org/10.1029/2009JD013642.

Rasmusson, E. M., & Carpenter, T. H. (1982). Variations in Tropical Sea Surface Temperature and Surface Wind Fields Associated with the Southern Oscillation/El Niño. *Monthly Weather Review.* https://doi.org/10.1175/1520-0493(1982)110<0354:VITSST>2.0.CO;2

Rayner, N. A, Parker, D. E, Horton, E. B, Folland, C. K., Alexander, L. V., Rowell, D. P., et al. (2003). Global analyses of sea surface temperature, sea ice, and night marine air temperature since the late nineteenth century. *Journal of Geophysical Research, 108*(D14), 4407. https://doi.org/10.1029/2002JD002670

Sui, C. H., Chung, P. H., & Li, T. (2007). Interannual and interdecadal variability of the summertime western North Pacific subtropical high. *Geophysical Research Letters, 34,* L11701. https://doi.org/10.1029/2006GL029204

Tan W, Wang, X., Wang, W. Q., Wang, C. Z., & Zuo, J. C. (2016). Different responses of Sea Surface Temperature in the South China Sea to various El Niño events during boreal autumn. *Journal of Climate*, *29,* 1127-1142. https://doi.org/10.1175/JCLI-D-15-0338.1

Trenberth, K. E., Branstator, G. W., Karoly, D., Kumar, A., Lau, N. C., & Ropelewski, C. (1998). Progress during toga in understanding and modeling global teleconnections associated with tropical sea surface temperatures. *Journal of Geophysical Research-Oceans, 103,* 14291-14324. https://doi.org/10.1029/97JC01444.

Wang, B., Wu, R., & Fu, X. (2000). Pacific–East Asian teleconnection : How does ENSO affect East Asian climate ? *Journal of Climate, 13,* 1517–1536.

https://doi.org/10.1175/1520-0442(2000)013<1517:PEATHD>2.0.CO;2

Wang, B., & Zhang, Q. (2002). Pacific–East Asian teleconnection. Part II: How the Philippine Sea anomalous anticyclone is established during El Niño development. *Journal of Climate*, *15*, 3252–3265. https://doi.org/10.1175/1520-0442(2002)015<3252:PEATPI>2.0.CO;2

Wang, C., & Wang, X. (2013). Classifying El Niño modoki I and II by different impacts on rainfall in southern China and typhoon tracks. *Journal of Climate*, *26*(4), 1322–1338. https://doi.org/10.1175/JCLI-D-12-00107.1

Wang, X., & Wang, C. (2014). Different impacts of various El Niño events on the Indian Ocean Dipole. *Climate Dynamics*, *42*(3–4), 991–1005. https://doi.org/10.1007/s00382-013-1711-2

Wang, X., Zhou, W., Li, C., & Wang, D. (2014) Comparison of the impact of two types of El Niño on tropical cyclone genesis over the South China Sea. *Int. J. Climatol.*, 34, 2651-2660. https://doi.org/10.1002/joc.3865.

Wang, X., Tan, W., & Wang, C. (2018a) A New Index for Identifying Different Types of El Niño Modoki Events. *Climate Dynamics*, 50 (7), 2753-2765. https://doi.org/10.1007/s00382-017-3769-8

Wang, X., Chen, M., Wang, C., Yeh, S. W., & Tan, W. (2018b) Evaluation of the relationships between the North Pacific Oscillation and El Niño Modoki in CMIP5 models. *Climate Dynamics.* https://doi.org/10.1007/s00382-018-4196-1

Wu, L., Wang, B., & Geng, S. (2005). Growing typhoon influence on east Asia. *Geophysical Research Letters, 32,* L18703. https://doi.org/10.1029/2005GL022937

Xiang, B., Wang, B., Yu, W., & Xu S. (2013). How can anomalous western North Pacific Subtropical High intensify in late summer? *Geophysical Research Letters, 40,* 2349–2354. https://doi.org/10.1002/grl.50431

Xie, S. P., Hu, K., Hafner, J., Tokinaga, H., Du, Y., Huang, G., & Sampe, T. (2009). Indian Ocean capacitor effect on Indo–western Pacific climate during the summer following El Niño. *Journal of Climate*, *22*, 730–747. https://doi.org/10.1175/2008JCLI2544.1

Xie, S. P., Kosaka, Y., Du, Y., Hu, K. M., Chowdary, J. S., & Huang, G. (2016). Indo-western Pacific ocean capacitor and coherent climate anomalies in post-ENSO summer: A review. *Advances in Atmospheric Sciences*, *33*(4), 411–432. https://doi.org/10.1007/s00376-015-5192-6

Yang, S., Li, Z., Yu, J. Y., Hu, X., Dong, W., & He, S. (2018). El Niño-Southern Oscillation and Its Impact in the Changing Climate. *National Science Review*, nwy046. https://doi.org/10.1093/nsr/nwy046

Yu, J. Y., & Kao, H. Y. (2007). Decadal changes of ENSO persistence barrier in SST and ocean heat content indices: 1958-2001. *Journal of Geophysical Research, 112*, D13106. https://doi.org/10.1029/2006JD007715

Yu, J. Y., Sun, F., & Kao, H. Y. (2009). Contributions of Indian Ocean and monsoon biases to the excessive biennial ENSO in CCSM3. *Journal of Climate*, *22*(7), 1850–1858. https://doi.org/10.1175/2008JCLI2706.1

Yu, J. Y., Kao, H. Y., & Lee, T. (2010). Subtropics-Related Interannual Sea Surface Temperature Variability in the Central Equatorial Pacific. *Journal of Climate*, *23*(11), 2869–2884. https://doi.org/10.1175/2010JCLI3171.

Yu, J. Y., & Kim, S. T. (2011). Relationships between extratropical sea level pressure variations and the central Pacific and eastern Pacific types of ENSO. *Journal of Climate*, *24*(3), 708–720. https://doi.org/10.1175/2010JCLI3688.1

Yu, J. Y., Zou, Y., Kim, S.T., & Lee, T. (2012). The Changing Impact of El Niño on US Winter Temperatures. *Geophysical Research Letters*, *39*, L15702. https://doi.org/10.1029/2012GL052483

Yu, J. Y., Paek, H., Saltzman, E. S., & Lee, T. (2015). The early 1990s change in ENSO-PSA-SAM relationships and its impact on Southern Hemisphere climate. *Journal of Climate*, *28*(23), 9393–9408. https://doi.org/10.1175/JCLI-D-15-0335.1

Yu, J. Y., Wang, X., Yang, S., Paek, H., & Chen, M. (2017). In S.-Y. Wang, J.-H. Yoon, C. Funk, & R. R. Gillies (Eds.), Changing El Niño–Southern Oscillation and associated climate extremes, book chapter in climate extremes: Patterns and mechanisms, *Geophysical Monograph Series* (Vol. 226, pp. 3–38). Washington, DC: American Geophysical Union

Yuan, Y., & Yang, S. (2012). Impacts of different types of El NiñO on the East Asian climate: Focus on ENSO cycles. *Journal of Climate*, *25*(21), 7702–7722. https://doi.org/10.1175/JCLI-D-11-00576.1

Yuan, Y., Yang, S., & Zhang, Z. (2012). Different evolutions of the philippine sea anticyclone between the eastern and central Pacific El Niño: Possible effects of Indian Ocean SST. *Journal of Climate*, *25*(22), 7867–7883. https://doi.org/10.1175/JCLI-D-12-00004.1

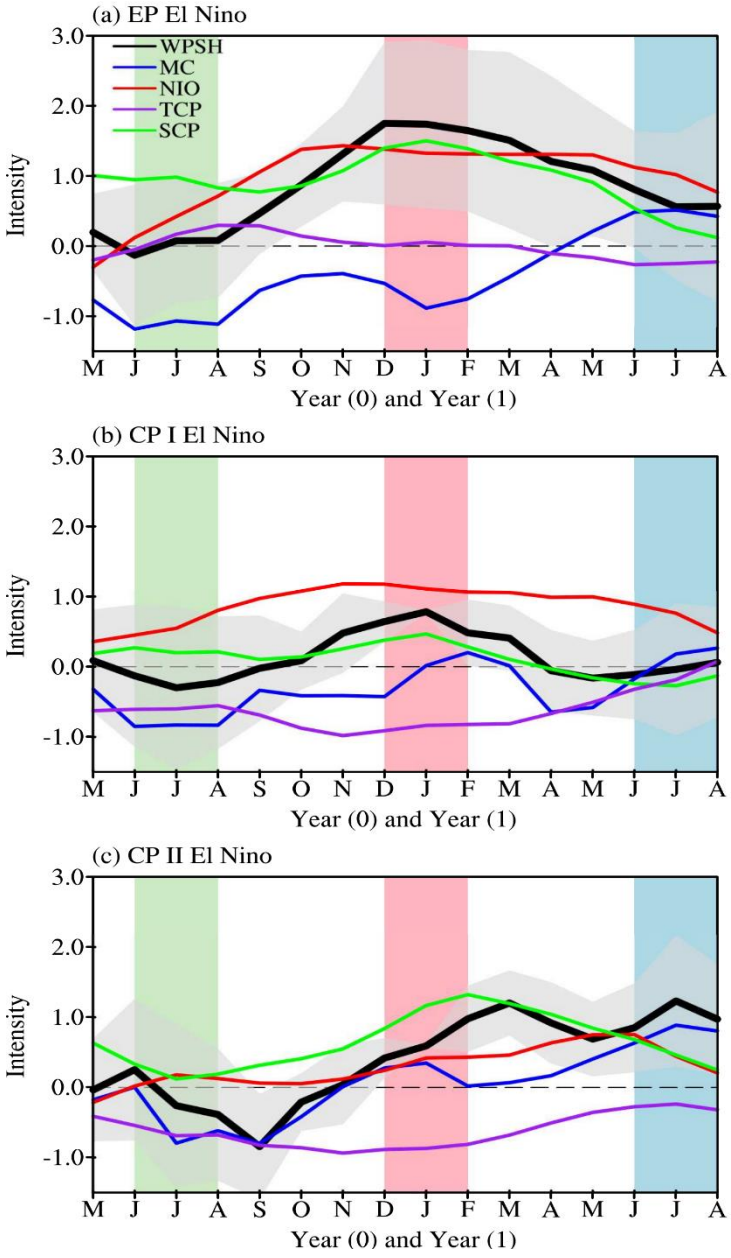

Figure 1. Composited standardized 3-month running mean Western Pacific subtropical high (WPSH) index (thick black), Maritime continent (MC) index (blue), Northern India Ocean (NIO) index (red), tropical central Pacific (TCP) index (purple) and subtropical central Pacific (SCP) index (green) during the developing and decaying year of (a) the EP El Niño, (b) the CP-I El Niño and (c) the CP-II El Niño. The gray shading indicates the range of one standard deviation.

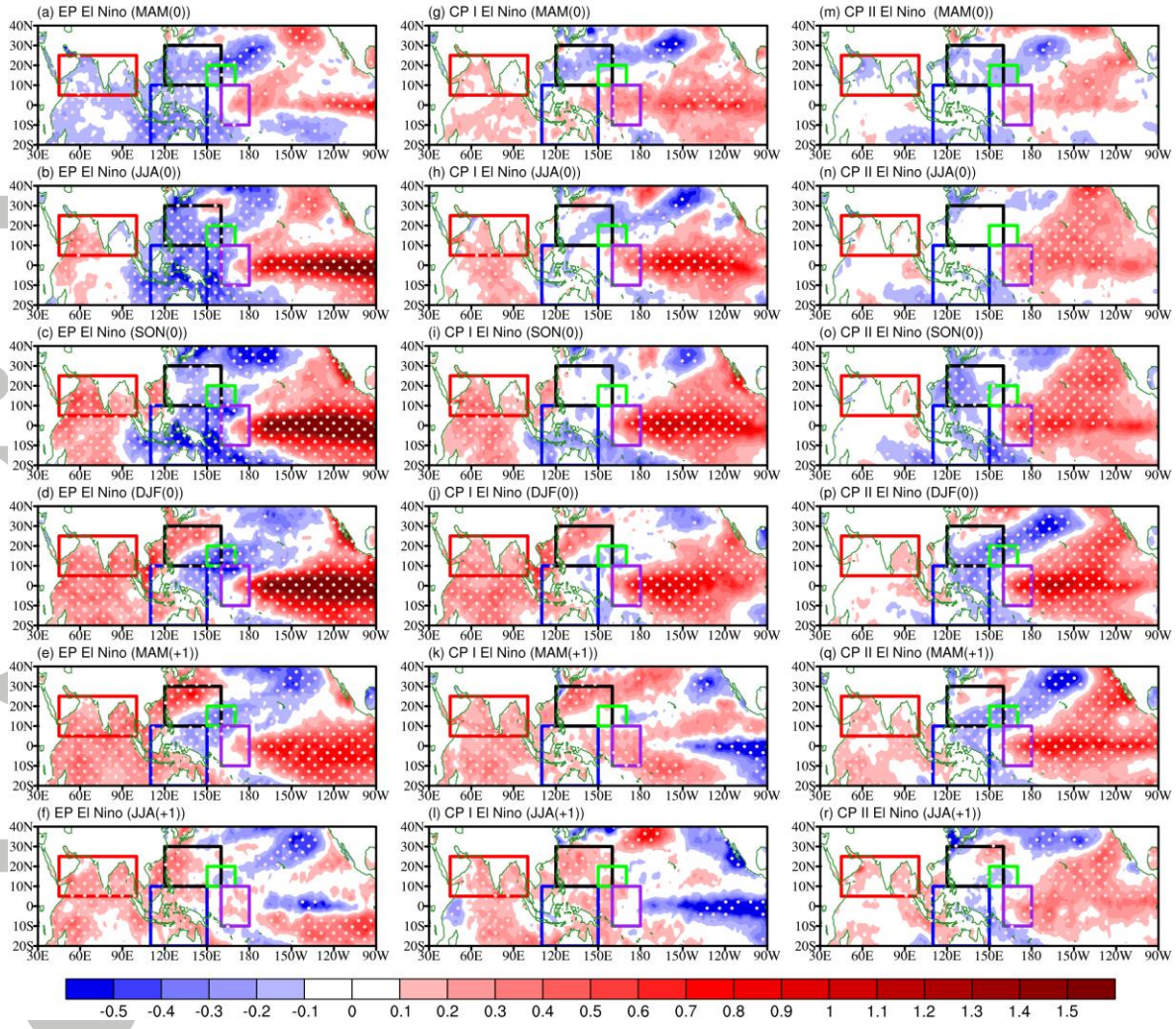

Figure 2. Evolution of composited SSTs (shaded, unit: ℃) for the EP El Niño (left column), the CP-I El Niño (middle column), and the CP-II El Niño (right column). The first, second, third, fourth and fifth rows represent the developing El Niño phases of MAM (March(0) to May(0)), JJA (June(0) to August(0)), DJF (December(0) to February(+1)), and decaying phases of MAM (March(+1) to May(+1), JJA (June(+1) to August(+1)), respectively. The black, blue, red, purple and green boxes represent the following regions: western North Pacific, maritime continent, Northern Indian Ocean, the region used to define the TCP index and the region used to define SCP index, respectively. The dotted regions represent the composite anomalies exceeding the 90 % significance level, which is calculated using a Student's t test.

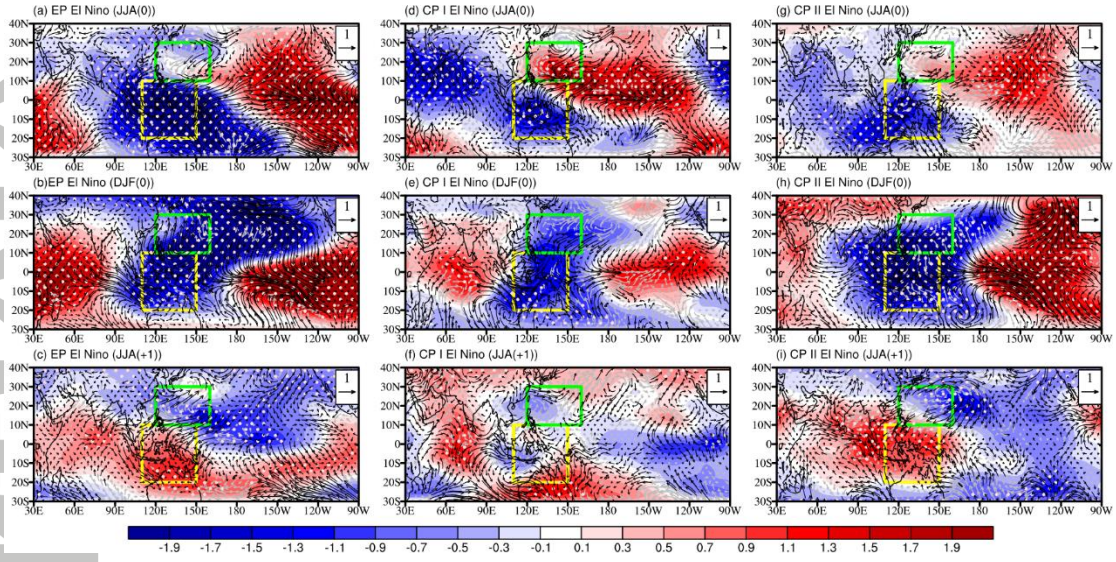

Figure 3. Composited 1000 hPa velocity potential anomalies (shaded, unit: $10^6 m^2 s^{-1}$) and 1000 hPa wind anomalies (vectors, unit: ms^{-1}) for the EP El Niño (the left column), the CP-I El Niño (the middle column), and the CP-II El Niño (the right column). The first, second and third rows represent the developing El Niño phases of JJA (June[0] to August[0]), DJF (December[0] to February[+1]) and decaying phase of JJA (June[+1] to August[+1]), respectively. The green and yellow boxes represent the regions of western North Pacific and maritime continent, respectively. The dotted regions represent the composite anomalies exceeding the 90 % significance level, which is calculated using a Student's t test.

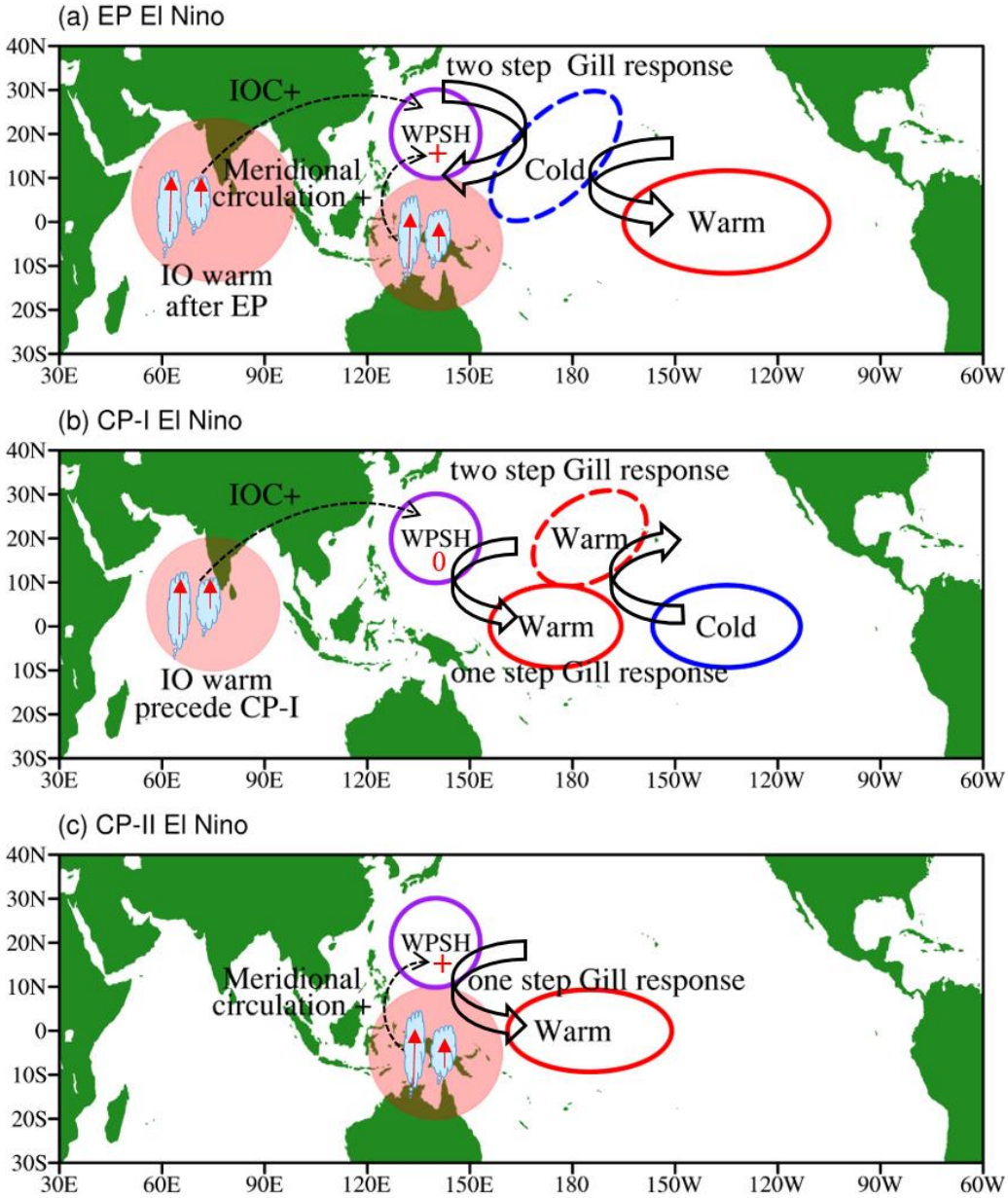

Figure 4. Schematic diagram showing the delayed impact mechanisms associated with the three types of El Niño on the Western Pacific Subtropical High. "0" and "+" of WPSH mean the SLP anomalies over WNP area are zero and positive, respectively. (a), (b) and (c) represent the EP El Niño, the CP-I El Niño and the CP-II El Niño, respectively.